

Beyond translesion synthesis: polymerase κ fidelity as a potential determinant of microsatellite stability

Suzanne E. Hile¹, Xiaoxiao Wang², Marietta Y. W. T. Lee² and Kristin A. Eckert^{1,*}

¹Department of Pathology, Gittlen Cancer Research Foundation, Pennsylvania State University College of Medicine, 500 University Drive, Hershey, PA 17033, ²Department of Biochemistry and Molecular Biology, New York Medical College, Valhalla, NY 10595, USA

Received August 26, 2011; Revised September 29, 2011; Accepted September 30, 2011

ABSTRACT

Microsatellite DNA synthesis represents a significant component of human genome replication that must occur faithfully. However, yeast replicative DNA polymerases do not possess high fidelity for microsatellite synthesis. We hypothesized that the structural features of Y-family polymerases that facilitate accurate translesion synthesis may promote accurate microsatellite synthesis. We compared human polymerases κ (Pol κ) and η (Pol η) fidelities to that of replicative human polymerase δ holoenzyme (Pol δ 4), using the *in vitro* HSV-*tk* assay. Relative polymerase accuracy for insertion/deletion (indel) errors within 2–3 unit repeats internal to the HSV-*tk* gene concurred with the literature: Pol δ 4 \gg Pol κ or Pol η . In contrast, relative polymerase accuracy for unit-based indel errors within [GT]₁₀ and [TC]₁₁ microsatellites was: Pol κ \geq Pol δ 4 $>$ Pol η . The magnitude of difference was greatest between Pols κ and δ 4 with the [GT] template. Biochemically, Pol κ displayed less synthesis termination within the [GT] allele than did Pol δ 4. In dual polymerase reactions, Pol κ competed with either a stalled or moving Pol δ 4, thereby reducing termination. Our results challenge the ideology that pol κ is error prone, and suggest that DNA polymerases with complementary biochemical properties can function cooperatively at repetitive sequences.

INTRODUCTION

Repetitive DNA sequences make up at least 50% of the human genome, and many correspond to a DNA structural complexity that is not found in other regions of the genome (1). Microsatellites, one type of interspersed

tandem repeat, are ubiquitous throughout the genome (2) and can be important functional regulators of gene expression and phenotypic variability (3). Microsatellite allele length polymorphisms have been implicated as genetic risk factors in human disease (4,5), and expansions at specific microsatellites are responsible for at least 40 inherited human disorders (6). Despite their importance for genome function and disease association, the fidelity mechanisms needed to maintain repetitive sequence stability have not been fully elucidated.

Stability of the eukaryotic genome requires the cooperative activity of multiple DNA polymerases (7,8). The Y-family DNA polymerases are a distinct group of enzymes and are present in bacteria, archaea and eukarya species (9). Initial biochemical characterization of the eukaryotic enzymes focused on their involvement in translesion synthesis (TLS), guided by the homology of eukaryotic genes to *Escherichia coli* genes that are involved in the DNA damage response. The identification of Pol η as the gene product affected in xeroderma pigmentosum-variant patients (10), together with the biochemical demonstration that Pol η promotes error-free bypass of several types of DNA lesions (11,12), solidified the concept that eukaryotic Y-family polymerases promote genetic stability through accurate TLS. Y-family polymerases can be distinguished by their substrate preferences, in that the enzymes catalyze error-free TLS for a variety of DNA lesions but with differential efficiencies (7). For example, Pol κ has been implicated in the accurate bypass of adducts at the exocyclic N² position of guanine, such as benzo[a]pyrene diol-epoxide (13) and furfuryl (14) lesions. The abilities of Pols κ and η to catalyze DNA synthesis past specific DNA lesions with high fidelity demonstrates that inherent polymerase accuracy is dependent upon the structure of the DNA substrate.

More recently, several investigations have garnered support for more widespread roles of Y-family polymerases in genome function. Human cells deficient in Pol η

*To whom correspondence should be addressed. Tel: +1 717 531 4065; Fax: +1 717 531 5634; Email: kae4@psu.edu

display aberrant S-phase progression and increased chromosomal fragility in the absence of exogenous exposure to DNA damaging agents (15). Genetic knock-down of Pol η or Pol κ increases the sensitivity of human cells to telomestatin, a compound that stabilizes G tetraplex DNA secondary structures (16). In human fibroblasts, complete DNA synthesis associated with nucleotide excision repair requires both Pol κ and Pol δ as well as Pol ϵ (17). The spontaneous germline mutation rate within two highly repetitive, expanded short tandem repeat alleles is higher for Pol κ -deficient mice, relative to isogenic Pol κ wild-type mice (18). Although limited, these studies suggest that Y-family polymerases have roles in genome maintenance beyond TLS.

DNA polymerases δ and ϵ are generally assumed to be responsible for the bulk of DNA replication as well as DNA synthesis associated with repair and recombination (19). These polymerases display highly accurate *in vitro* DNA synthesis using undamaged DNA templates (20,21). However, we reported that the replicative holoenzyme forms of yeast Pol δ and Pol ϵ do not possess high fidelity during *in vitro* microsatellite DNA synthesis (22). Because Y-family polymerases perform accurate TLS of specific lesions, we hypothesized that the structural or biochemical features underlying accurate TLS may also allow increased polymerase discrimination of alternative DNA structures, such as those formed by repetitive microsatellite sequences. In this study, we demonstrate that the human Y-family polymerase, Pol κ , displays a high accuracy during dinucleotide microsatellite DNA synthesis. We postulate that accurately maintaining microsatellites and possibly other repeated DNA

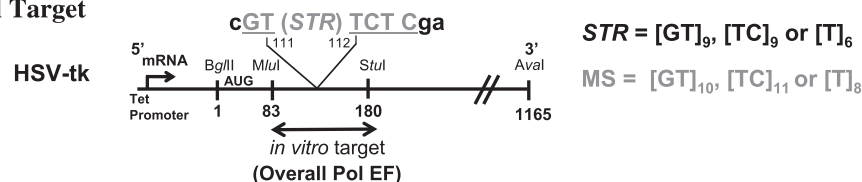
sequences may be an additional cellular function for specialized DNA polymerases.

MATERIALS AND METHODS

In vitro gap-filling HSV-*tk* mutagenesis assay

The 4-subunit recombinant human Pol δ 4 and proliferating cell nuclear antigen (PCNA) were purified as described (23). Purified full-length Pol κ (99 kDa) and Pol η (78 kDa) were purchased from Enzymax (Lexington, KY, USA). Microsatellite-containing Herpes simplex virus type 1 thymidine kinase (HSV-*tk*) vectors have been previously described (24,25). The *Mlu*I (position 83) to *Stu*I (position 180) HSV-*tk* target sequence within the gapped duplex (GD) molecule contains 89–91 bp of HSV-*tk* gene coding region sequence, and 8 bp ([T]₈), 20 bp ([GT]₁₀), or 22 bp ([TC]₁₁) of microsatellite sequence (Figure 1A). *In vitro* gap-filling reactions (Figure 1B) contained 0.075–0.125 pmol of gapped substrate and 250 μ M deoxynucleotide triphosphates (dNTPs) in 100 μ l final volume. Pol δ 4 reactions contained 40 mM Tris pH 7.8, 10 mM MgCl₂, 1 mM DTT, 5 mM NaCl, 200 μ g/ml BSA and 1.2–4 pmol pol δ 4. Pol δ 4 reactions containing accessory factors were supplemented with 2 mM ATP, 40 ng (450 fmol) PCNA and 5 ng (17 fmol) replication factor C (RFC). Reactions were incubated at 37°C for 30 min–1 h. Pol κ and Pol η reactions contained 25 mM potassium phosphate buffer pH 7.2, 5 mM MgCl₂, 5 mM DTT, 100 μ g/ml BSA, 10% glycerol and 1.9–9.4 pmol of polymerase. Reactions were incubated at 37°C for 2 h. All reactions were terminated with 15 mM

A HSV-*tk* Mutational Target



B Schematic of Experimental Approach

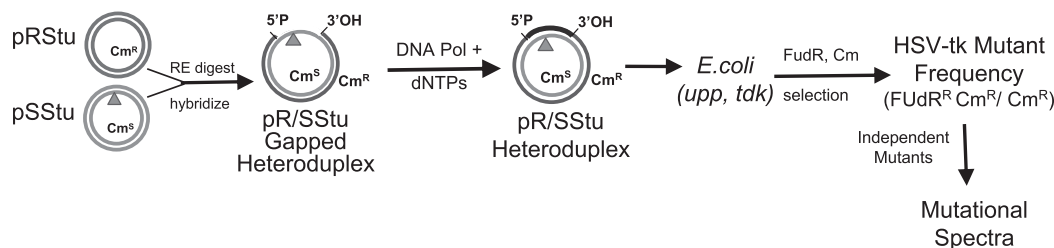


Figure 1. Schematic of the HSV-*tk* experimental system. (A) HSV-*tk* mutational target. Short tandem repeat (STR) sequences were inserted in-frame between bases 111 and 112 of the HSV-*tk* mutational target to create artificial microsatellites (MS). Inactivating mutations can arise within the MS sequence (MS mutation frequency in Tables 1 and 2), as well as within the approximately 100 base pair region (*Mlu*I–*Stu*I) of the *in vitro* HSV-*tk* gene mutational target (HSV-*tk* coding mutation frequency in Tables 1 and 2). The sum of these mutations is shown as the overall Pol EF in Tables 1 and 2. (B) Cartoon of experimental approach. HSV-*tk* gene cassettes were cloned into two sister plasmids, one of which encodes a functional chloramphenicol acetyltransferase (*cat*) gene (pRStu) and one which encodes a nonfunctional *cat* gene (pSSStu) (24,25). The location of the MS sequences is indicated by an inverted triangle. Gapped heteroduplex molecules were created by hybridizing the *Mlu*I–*Stu*I large fragment from the pRStu vector to ssDNA derived from pSSStu vectors. Gel purified gapped substrates were used as templates for DNA synthesis reactions containing purified human DNA polymerases. Product DNAs were introduced into *E. coli* (*upp*, *tdk*) for mutational analyses. Chloramphenicol (Cm) selects for bacteria derived from the heteroduplex Cm^R strand; FUDR selects for HSV-*tk*-deficient bacteria. DNA sequence changes of independent FUDR^R mutants are determined to derive a mutational spectrum.

Ethylenediaminetetraacetic acid (EDTA), and exchanged into Tris-EDTA (TE) buffer. Complete gap filling by all three polymerases was verified as described (22) (Supplementary Figure S1). An aliquot of DNA from complete gap-filling reactions was used to transform *E. coli* strain FT334 for mutant frequency determination (26) (Figure 1B). To control for pre-existing mutations, we also determined the HSV-tk mutant frequencies (MF) for each ssDNA used to construct the GD molecules. The DNA sequences within the target region of independent mutants isolated from 2 to 3 polymerase reactions per template were determined (24).

Determination of polymerase error frequencies

Pol η and Pol κ produced multiple mutational events per target sequence, while Pol δ normally created only 1 mutational event per target. In order to properly compare error rates among these three polymerases, we identified those mutational events that were detectable as single mutational events, and adjusted the HSV-tk MF to reflect multiple errors per target. First, polymerase error frequencies (Pol EFs) were determined by the following equation: Pol EF = (Observed MF) – (ssDNA background MF) – (Outside target MF) where outside target MF is the frequency of errors occurring outside the gap target, either through background errors in the GD molecule, polymerase displacement synthesis or polymerase exonuclease activity (Pol δ). Next, the Pol EF was adjusted by performing calculations as described (27) with a few modifications. Each mutational event was scored as detectable or undetectable. All frameshifts and those base substitutions that changed an amino acid were considered detectable. Each mutational event was also scored as tandem or non-tandem. Tandem events were those adjacent to one another, whereas non-tandem were errors >1 nt apart. To fully represent all of the mutational events created by the human polymerases, both detectable and undetectable events within the HSV-tk gene are depicted in Supplementary Figure S2. However, only those that were detectable were used for determining Pol EF_{est}. Pol EFs were then corrected for the existence of multiple mutations according to the following formula:

$$\text{Pol EF}_{\text{est}} = \text{Pol EF} / \sum_{n=1}^4 (1/n) (\text{mutants with } n \text{ errors} / \text{total analyzed mutants})$$

where n is the number of detectable non-tandem errors. The Pol EF_{est} of a specific type of mutational event was calculated from the proportion of the specific mutational event (among the total analyzed) multiplied by Pol EF_{est}.

Pol δ and Pol κ primer extension competition analyses

In a common buffer (25 mM potassium phosphate buffer pH 7.2, 5 mM MgCl₂, 2.5 mM DTT, 200 μ g/ml non-acetylated BSA and 250 μ M dNTPs), Pol κ is 4- to 5-fold more active than Pol δ in the absence or presence of PCNA, using circular ssDNA as the template (Supplementary Figure S3, panel B). Primer extension

analyses were performed to determine termination within a [GT]₁₀ microsatellite for Pol δ and Pol κ individually and together in a competition assay. Primer IHTW02, a 15-mer oligonucleotide that initiates synthesis at HSV-tk position 132 was radioactively 5' end-labeled and hybridized to [GT]₁₀-containing ssDNA as described (28). Reactions containing 100 fmol of primed substrate and the common buffer in a final volume of 20 μ l were preincubated at 37°C for 3 min. Synthesis was initiated upon addition of Pol κ or equivalent activity of Pol δ . Aliquots were removed at 5, 15 and 30 min and quenched as described (28). Reaction products were separated on an 8% denaturing polyacrylamide gel and quantitated using a Molecular Dynamics Phosphorimager. The number of DNA molecules within three regions (5' to the [GT]₁₀ microsatellite, the [GT]₁₀ microsatellite, and 3' to the [GT]₁₀ microsatellite) were determined by ImageQuant software and corrected for background and loading differences. [GT]₁₀ termination probability is defined as the number of molecules within the [GT]₁₀ microsatellite divided by the number of molecules within the [GT]₁₀ microsatellite and 3' to the [GT]₁₀ microsatellite. Polymerase competition assays were performed similarly with 400 fmol of Pol δ \pm 500 fmol PCNA, initiating synthesis in either moving (with 250 μ M dNTPs) or stalled (-dATP) conditions. After 5 min, 40 fmol of Pol κ or an equivalent activity of Pol δ (200 fmol; thus, 600 fmol Pol δ final) was added (along with a final concentration of 250 μ M dATP in the stalled reactions). Quantitation of reaction products was performed as above.

RESULTS

To measure the frequency and types of mutational events within repetitive DNA, we engineered the 5'-region of the HSV-tk gene to contain a variety of in-frame, short microsatellite (MS) sequences (Figure 1A). Gapped DNA heteroduplex molecules were constructed, and an *in vitro* DNA polymerase gap-filling assay was used to measure polymerase error rates within the *MluI* to *StuI* target (24). Forward mutations that inactivate the HSV-tk protein were scored after transfection of *E. coli* with the reaction products and selective plating (Figure 1B). An HSV-tk mutant phenotype can be generated either by mutations arising within the microsatellite motifs (that are not a multiple of three), or by mutations arising within the surrounding HSV-tk target coding sequence (Figure 1A). This experimental approach allows us to directly measure mutations in microsatellite alleles of varying sequence composition, and compare such events to mutations in the HSV-tk-coding sequence.

Replicative DNA polymerase fidelity within microsatellite alleles

We measured the fidelity of the recombinant 4-subunit holoenzyme form of human DNA polymerase δ (Pol δ). Polymerase reactions were performed using gapped DNA substrates containing [GT]₁₀, [TC]₁₁ or [T]₈ microsatellite reporter cassettes. The observed HSV-tk mutant frequencies for Pol δ were 8- to 44-fold higher than the

Table 1. Replicative DNA polymerase δ holoenzyme error rates within microsatellite and HSV-tk coding DNA sequences

Polymerase	Observed HSV-tk frequency ^a $\times 10^{-4}$ (\pm SD)	Pol EF _{est} $\times 10^{-4}$ ^b (No. mutational events observed)		
		Overall	HSV-tk coding ^c	Microsatellite ^c
pSStu2 / [GT] ₁₀ template				
None ^d	4.1	0.26 (3)	<0.087 (0)	0.26 (3)
Pol δ 4	32 \pm 5.2	27 (67)	4.0 (10)	23 (57)
Pol δ 4 + PCNA/RFC	41	31 (33)	5.6 (6)	25 (27)
pSStu4 / [TC] ₁₁ template				
None	3.5	2.0 (26)	<0.078 (0)	2.0 (26)
Pol δ 4	43 \pm 22	31 (62)	7.5 (15)	24 (47)
Pol δ 4 + PCNA/RFC	28	20 (24)	6.7 (8)	13 (16)
pSStu10 / [T] ₈ template				
None	0.89	ND	ND	ND
Pol δ 4	39 \pm 8.2	33 (32)	2.1 (2)	31 (30)

^aObserved mutant frequencies are mean of two, or mean \pm SD of 3–6 independent reactions.

^bPolymerase error frequency (Pol EF) was calculated using the equation: Pol EF = (Observed MF) – (ssDNA Background MF) – (Outside Target MF).

Pol EFs were adjusted for those mutants that had 2 or more mutational events in the target (see Methods). Mutants analyzed for DNA sequence changes were isolated from 2–3 independent polymerase reactions.

^cCoding and microsatellite PolEF_{est} were calculated by multiplying the proportion of mutational events at either site by the overall PolEF_{est}.

^dMutant frequency measured by electroporation of the ssDNA used to create the gapped DNA substrates. The corresponding overall Pol EF value is the frequency of mutations within the gapped target.

ND not determined.

ssDNA background frequency (Table 1). The observed HSV-tk mutant frequencies were adjusted for background and multiple mutational events after DNA sequence analyses to obtain the overall estimated polymerase error frequencies (overall Pol EF_{est}; Table 1). This overall PolEF_{est} is a result of polymerase errors within both the HSV-tk coding and microsatellite sequences of the target (Figure 1A). Polymerase error frequencies solely within the HSV-tk coding or the microsatellite sequences were calculated based on the proportion of mutational events within each of these regions. The majority (76–94%) of human Pol δ 4 errors were produced within the microsatellite sequences for all three substrates (Table 1). The Pol EF_{est} for Pol δ 4 errors was high within the [GT]₁₀ (2.3×10^{-3}), [TC]₁₁ (2.4×10^{-3}), and [T]₈ (3.1×10^{-3}) alleles. We examined whether the PCNA/RFC complex could specifically increase Pol δ 4 fidelity at microsatellite sequences. Pol δ 4 fidelity within either the HSV-tk-coding sequences or the [GT]₁₀ and [TC]₁₁ microsatellites was not altered by the addition of PCNA and RFC (Table 1). An earlier study showed that these accessory proteins lower yeast Pol δ fidelity for base substitution errors (29).

Y-family DNA polymerase fidelity within microsatellites

We tested our hypothesis that microsatellite mutagenesis may vary with respect to DNA polymerase families, using human Y-family polymerases. Under our experimental buffer and template conditions, Pol κ and Pol η display similar or better DNA synthesis efficiencies to that of Pol δ 4 (Supplementary Figure S3 and data not shown). The observed HSV-tk mutant frequencies for Pol κ and Pol η reactions were 3- to 16-fold higher than Pol δ 4 for each template (Table 2). As a control, we compared the relative accuracy of the three polymerases during synthesis of the HSV-tk-coding sequences. The average coding Pol EF_{est}

was 4.5×10^{-4} for Pol δ 4, 120×10^{-4} for Pol κ , and 380×10^{-4} for Pol η (Supplementary Table S1). Thus, Pol κ and Pol η are, on average, 27- and 84-fold less accurate than Pol δ 4 at coding sequences, respectively. These data are in complete agreement with published results using the lacZ target and purified proteins from other sources (30–32).

When comparing polymerase fidelity at microsatellite sequences, we observed a low Pol κ error rate for mutations arising within the [GT]₁₀ and [TC]₁₁ dinucleotide sequences (Table 2). Remarkably, the Pol κ error frequency measured within dinucleotide alleles is 4- to 8-fold lower than the frequency of errors within the HSV-tk-coding region. Moreover, within these two microsatellite alleles, Pol κ does not display an error-prone phenotype, as the Pol EF_{est} for Pol κ is not higher than that for Pol δ 4 (Tables 1 and 2). This selective accuracy is specific for Pol κ and not a general feature of Y-family polymerases, since the Pol EF_{est} for dinucleotide errors produced by Pol η is high for both microsatellite alleles (Table 2).

The creation of microsatellite interruptions by human DNA polymerases

Various types of errors can be produced by polymerases within dinucleotide microsatellite alleles (33), and can be broadly classified into either unit-based insertion/deletion (indel) errors (where 2 nt is the unit size for dinucleotide repeats), or interruption errors (Figure 2A). Microsatellite unit-based indel errors characterize the mutational behavior of microsatellites observed in numerous model systems. If left uncorrected, such errors will result in allele length changes that can be a source of genomic instability (3). Interruption errors are any error that disrupts the tandem repeat sequence, converting the repetitive tract from one that is pure to one that is impure. Such errors in dinucleotide alleles can occur via multiple

Table 2. Y Family DNA polymerase error rates within microsatellite and HSV-tk coding DNA sequences

Polymerase	Observed HSV-tk frequency ^a $\times 10^{-4}$ (\pm SD)	Pol EF _{est} $\times 10^{-4b}$ (No. mutational events observed)		
		Overall	HSV-tk coding ^c	Microsatellite ^c
pSStu2 / [GT] ₁₀ template				
Pol κ	140 \pm 67	160 (160)	140 (144)	16 (16)
Pol η	460 \pm 52	410 (100)	320 (79)	86 (21)
pSStu4 / [TC] ₁₁ template				
Pol κ	120 \pm 39	100 (75)	80 (60)	20 (15)
Pol η	680 \pm 120	710 (130)	430 (78)	280 (52)
pSStu10 / [T] ₈ template				
Pol κ	430 \pm 85	460 (49)	140 (15)	320 (34)
Pol η	430 \pm 140	440 (35)	210 (17)	230 (18)

^aMutant frequencies are mean \pm standard deviation of 3–6 independent reactions.

^{b,c}See legend to Table I for derivation of values.

Bold values indicate a low Pol κ error frequency for mutations arising within the [GT]₁₀ and [TC]₁₁ sequences.

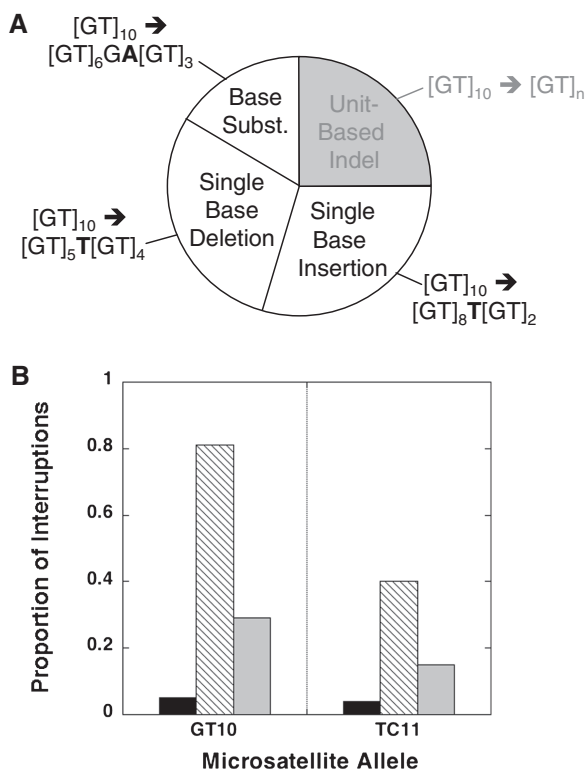


Figure 2. Specialized Y-family polymerases Pol κ and Pol η create more interruptions in dinucleotide microsatellites than does Pol $\delta 4$. (A) Types of mutations arising within dinucleotide microsatellites. Mutations within the dinucleotide microsatellite can occur via unit-based indel events (gray area) or by interruption events (white areas). Examples of interruption events by single base insertion, single base deletion, and base substitution mechanisms are shown for the [GT]₁₀ allele. (B) Graphs depict the proportion of microsatellite interruptions among the total number of microsatellite mutational events at the [GT]₁₀ and [TC]₁₁ alleles for Pol $\delta 4$ (solid bars), Pol κ (hatched bars) and Pol η (gray bars).

mechanisms, including single base indel or base substitution errors (Figure 2A). Although interruptions are polymerase errors, such errors are expected to be less detrimental genetically than unit-based indel errors. First, interruptions are known to stabilize expanded

microsatellites (6). Second, microsatellite interruptions can divide the sequence into two smaller alleles with lengths below the threshold (34), thereby lowering mutability and initiating microsatellite degeneration.

We compared the propensity for the three polymerases to create interruption errors *in vitro*. The replicative Pol $\delta 4$ enzyme created very few interruptions within the alleles examined (Figure 2B). In stark contrast, Pol κ produced many interruption errors (up to 81%) within the GT₁₀ and TC₁₁ alleles, which is significantly different from Pol $\delta 4$ ($P \leq 0.0001$ and $P = 0.002$, respectively, Fisher's exact test, Figure 2B). Thus, the Pol κ error frequency within the dinucleotide alleles is low (Table 2), and the few errors that are made by Pol κ are often interruptions, which may have beneficial consequences.

Distinct polymerase fidelity of unit-based indels within microsatellites

Both unit-based microsatellite allele length changes and traditional frameshift errors within coding sequences arise by a strand misalignment mechanism. Therefore, to directly compare the likelihood of the two types of polymerase misalignment errors, we calculated the Pol EF_{est} for indel errors within the HSV-tk coding region versus unit-based indel errors within the microsatellite alleles.

The HSV-tk target sequence includes 23 'monitor' sites of short tandem repeats (19 mononucleotide and four dinucleotide repeats of 2–3 units in length) that provide a good portrayal of polymerase indel errors occurring within coding sequences (34; underlined sequences in Supplementary Figure S2). As the HSV-tk coding region Pol EF_{est} for each polymerase did not vary substantially between the different templates examined, a composite spectrum of coding region errors was created for each polymerase (Supplementary Figure S2). Strikingly, Pol κ produced primarily indel errors within monitor tandem repeats, as well as at non-repeated sequences. The Pol EF_{est} for Pol κ or Pol η indel errors within the HSV-tk coding region is ~ 100 -fold higher than the Pol EF_{est} for Pol $\delta 4$ (Figure 3A and Supplementary Table S1). These data establish that the hierarchy of polymerase accuracy for indel errors within short tandem repeats of coding sequences follows the order: Pol $\delta 4$ \gg Pol κ or Pol η . A

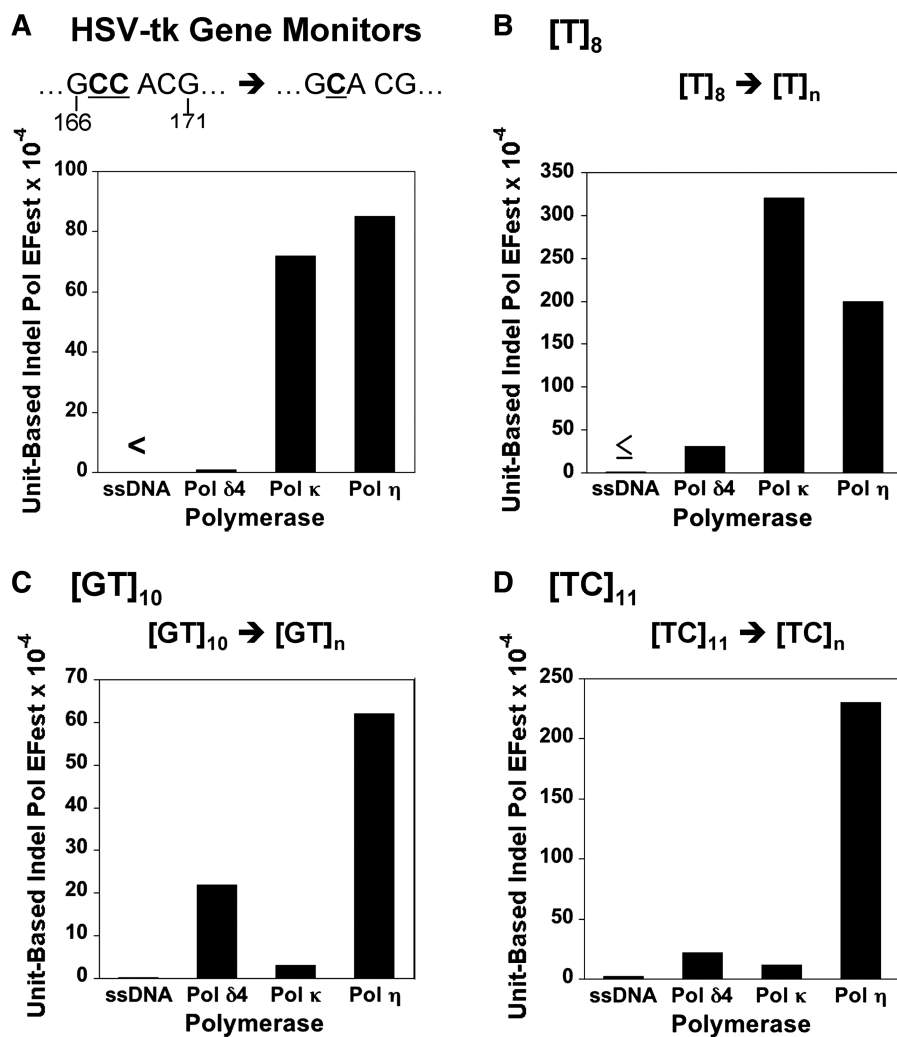


Figure 3. Comparison of DNA polymerase unit-based indel accuracy. (A) HSV-tk-coding sequence monitors. For each polymerase, the coding region polymerase error frequencies (from Tables 1 and 2) were averaged among all templates, and the combined proportion of indel errors at the 23 monitor sites versus all detectable mutational events was calculated. This proportion was multiplied by the average coding PolEF_{est} and the result graphed. One example of the type of mutations included in the analysis is depicted: the loss of one C residue within a short mononucleotide tandem repeat at HSV-tk positions 167–168. See Supplementary Figure S2 for complete representation of indel mutations at the 23 monitor sites. No mutational events were found at the coding region monitors among the mutants sequenced for the ssDNA background, and the error frequency is estimated to be $<0.08 \times 10^{-4}$. (B) [T]₈ mononucleotide repeat. Indels at [T]₈ are defined as any gain or loss of T units that change the length of the [T]₈ tract to [T]_n. The PolEF_{est} for [T]₈ indels was calculated by multiplying the proportion of MS unit indel errors by the MS PolEF_{est} (Tables 1 and 2) for each polymerase. Background mutants from [T]₈ ssDNA were not sequenced; therefore, the indel error frequency is $\leq 0.89 \times 10^{-4}$. (C) [GT]₁₀ microsatellite; and (D) [TC]₁₁ microsatellite sequences. Indels at [GT]₁₀ or [TC]₁₁ are defined as any gain or loss of dinucleotide units that change the length of the tract. The PolEF_{est} for [GT]₁₀ and [TC]₁₁ indels was calculated by multiplying the proportion of MS indel errors by the MS PolEF_{est} (Tables 1 and 2) for each template and polymerase.

similar result was observed for the relative accuracy of Pols δ4, κ and η during synthesis of the [T]₈ mononucleotide microsatellite allele. Specifically, Pols κ and η displayed a 10-fold higher Pol EF_{est} for unit-based errors within the allele than did Pol δ4 (Figure 3B).

A very different hierarchy of polymerase fidelity was observed for unit-based indel errors within both dinucleotide alleles. Pol δ4 produced almost exclusively (89–95%) unit-based indel errors (and correspondingly few interruptions; Figure 2B), resulting in a high unit-based indel error frequency (Figure 3C and D). In contrast, few unit-based indel errors were observed in the Pol κ error spectra, because Pol κ creates many interruptions (Figure 2B). Thus, the resulting Pol EF_{est} for unit-based indel errors

produced by Pol κ was lower than that produced by Pol δ4 in both dinucleotide alleles (Figure 3C and D).

To compare polymerase indel error rates among targets of differing repeat lengths, we calculated the Pol EF/unit, where the unit size is one for mononucleotide and two for dinucleotide repeats (Table 3). For Pol δ4, the GT microsatellite indel error rate is 100-fold higher than HSV-tk-coding indel error rate, demonstrating the inherent inaccuracy of Pol δ4 at microsatellites (Table 3). Quite the opposite is true for Pol κ, as the ratio of the indel error rate within the GT microsatellite versus the HSV-tk-coding sequence is 0.17 (Table 3). Within the TC allele, the Pol δ4 indel error rate/unit is 22×10^{-5} , and the Pol κ indel error rate/unit is 11×10^{-5} . Thus,

Table 3. The hierarchy of DNA polymerase accuracy for indel errors is substrate-dependent

Polymerase	Pol family	Indel polymerase error rate $\times 10^{-5}$		Ratio GT ₁₀ / HSV-tk
		HSV-tk coding ^a	[GT] ₁₀ ^b	
ypol ϵ^c	B	0.033	9.0	270
hpol δ	B	0.17	22	130
ypol δ^c	B	0.23	25	110
calf thymus pol α^d	B	1.9	19	10
rat pol β^e	X	3.3	8.4	2.5
hpol η	Y	13	62	4.8
hpol κ	Y	18	3.0	0.17

^aCoding indel monitor polymerase error rates are reported per unit and were determined by dividing the coding indel PolEF_{est} by the total number of mono- and dinucleotide units included in all monitor sites (total from target sequence is 48).

^b[GT]₁₀ indel polymerase error rates are reported per unit and were determined by dividing the microsatellite indel PolEF_{est} by the total number of GT units.

^cData from (22).

^dUnpublished data.

^eData from (24,34).

the ratio of polymerase error rates within the TC microsatellite/coding sequence is 130 for Pol δ , but only 0.7 for Pol κ . The similarity in rank order of polymerase fidelity for GT and TC motifs suggests that Pol κ accuracy may be similar to or greater than that of replicative polymerases at other dinucleotide alleles. Our data demonstrate that the hierarchy of DNA polymerase fidelity is dependent upon DNA substrate sequence, and for dinucleotide microsatellites, follows the alternative order: Pol $\kappa \geq$ Pol $\delta >$ Pol η .

Cooperativity between Pol δ and Pol κ at dinucleotide microsatellites

Using an *E. coli* model, Indiani *et al.* demonstrated that *E. coli* Pol IV can freely exchange with a moving replicative Pol III holoenzyme during DNA replication (35). In another model, an exchange between *Saccharomyces cerevisiae* Pol δ and Pol η was observed only upon stalling of the replicative polymerase (36). In both of these models, the polymerase exchange was monitored as a change in DNA synthesis rates and/or length of the DNA reaction products. Keeping these studies in mind, we ascertained whether Pol δ and Pol κ displayed polymerase-specific termination profiles within the GT₁₀ microsatellite that could be used to monitor polymerase exchange. The termination probability of Pol δ within the GT allele was determined at three different polymerase:DNA template ratios (Figure 4). Under limiting enzyme conditions (2.5:1, Pol δ :DNA ratio), we observed a high termination probability (0.76–0.84) within the [GT]₁₀ sequence at all time points (Figure 4B, top panel). With higher amounts of enzyme, the termination probability decreased with increasing reaction time (Figure 4B, bottom panel), suggesting the product accumulation observed within the [GT]₁₀ sequence is due to

slowing of Pol δ synthesis rather than an absolute inhibition. To directly compare polymerase synthesis profiles, we determined the specific activities of our preparations of Pol δ and Pol κ using both primer extension (ssDNA template containing a [GT]₁₀ sequence) and dTTP incorporation (poly dA/oligo dT primer-template) (Supplementary Figure S3). Under identical buffer conditions, Pol κ is 4- to 5-fold more active than Pol δ . Therefore, we examined Pol κ termination probability within the [GT]₁₀ sequence using 4–5-fold lower molar amounts of enzyme, relative to Pol δ (i.e. we compared equal activity). Under enzyme-limiting conditions (0.5:1, enzyme to DNA ratio), the Pol κ termination probability within the [GT]₁₀ sequence was 0.56–0.60, lower than Pol δ at all time points (Figure 4B, top panel). With increasing Pol κ amounts, termination probability again decreased with reaction time. More importantly, however, the Pol κ termination probability was significantly lower than the Pol δ termination probability for every time point examined ($P = 0.003$, 5 and 15 min; $P = 0.05$, 30 min; unpaired student *t*-test) (Figure 4B, middle panel).

The differential termination observed above within the GT allele allowed us to test whether Pol κ could alleviate microsatellite-specific Pol δ termination. In preliminary experiments, we observed a significant decrease in GT₁₀ termination when the synthesis reactions contained both Pol δ and Pol κ in similar molar amounts (0.5 pmol Pol δ and 0.25 pmol Pol κ), relative to reactions containing 0.75 pmol of Pol δ alone (Supplementary Figure S4). However, we also observed an appreciable increase in total primer-template extension in the dual polymerase reactions, relative to reactions with Pol δ alone. Because we also noted a difference in the specific activity of our two enzyme preparations (Supplementary Figure S3), we were concerned that using near equimolar polymerase amounts would give an unfair advantage to the more active polymerase preparation, in this case, Pol κ . Thus, we examined whether Pol κ could compete with Pol δ during microsatellite DNA synthesis using submolar amounts of Pol κ to control for specific activity differences. We examined two different experimental scenarios. In the first set of experiments, we allowed Pol δ to begin synthesis without any impediments, and then added either a 10-fold submolar amount of Pol κ , relative to Pol δ , or an equal activity of additional Pol δ (as a control). After quantitating the resultant termination probability within the [GT]₁₀ sequence, we observed that the amount of microsatellite-specific termination decreased when Pol κ was added to the reaction, relative to the Pol δ only reaction (Figure 5A). These results demonstrate that Pol κ can effectively compete with a moving Pol δ for primer-extension synthesis, even when Pol δ is present in a 10-fold molar excess over Pol κ . In the second set of experiments, we loaded Pol δ onto the DNA template in the presence of only three dNTP substrates in order to force Pol δ to stall prior to encountering the microsatellite sequence. Again, we added either Pol κ or an equal activity of additional Pol δ , along with dATP, and analyzed DNA synthesis progression through the microsatellite. We observed a decrease of the microsatellite-specific Pol δ pause with addition of as

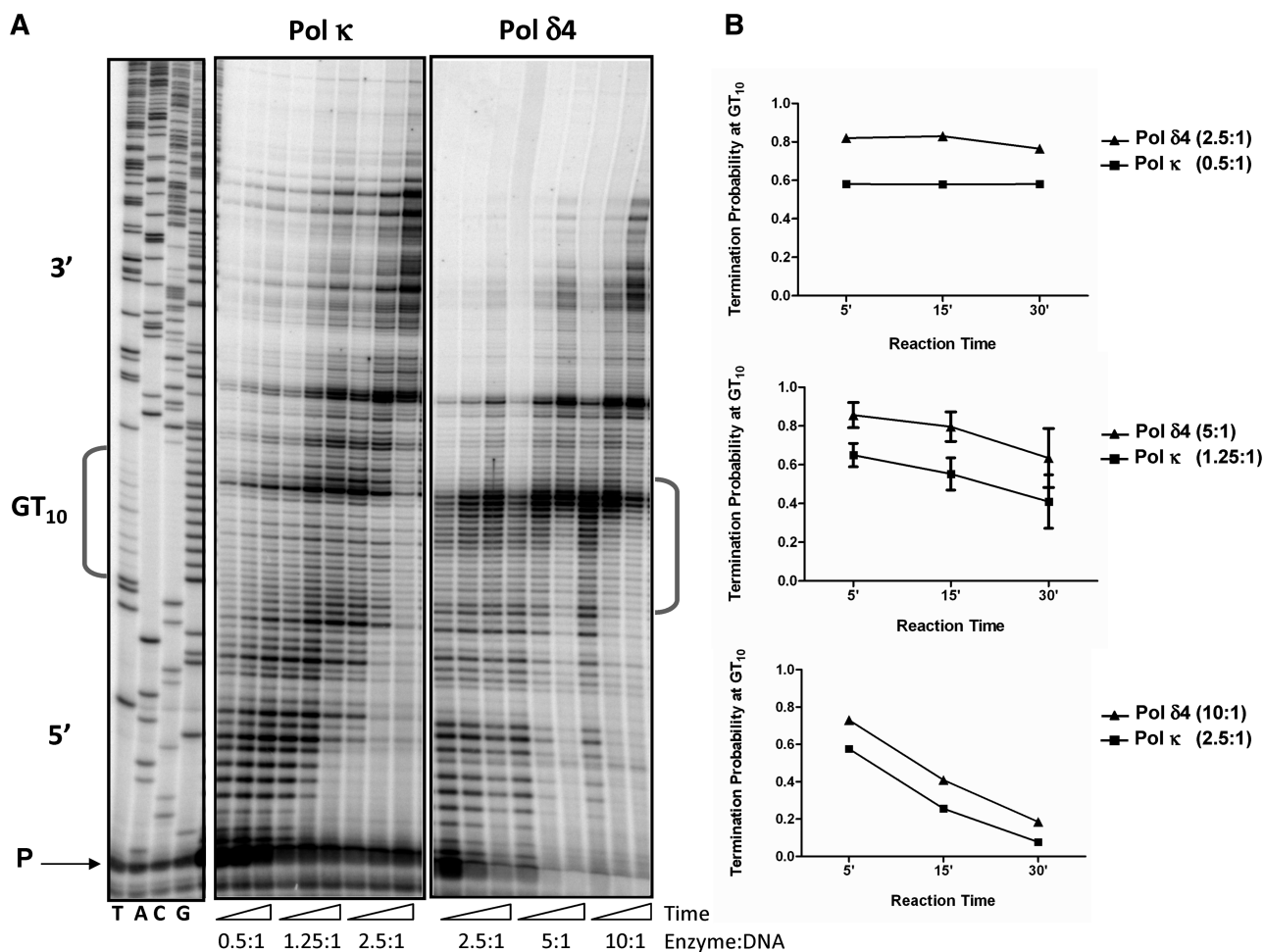


Figure 4. Differential termination of Pol $\delta 4$ and Pol κ DNA synthesis within the $[GT]_{10}$ microsatellite. (A) Representative phosphorimager scan of primer extension reaction products. The enzyme:DNA ratios for Pol κ (middle panel) and equivalent activity of Pol $\delta 4$ (right panel) are indicated. Triangles represent increasing reaction times (5, 15, 30 min). Reactions were run alongside a DNA sequencing ladder (left panel). (B) Quantitation of the reaction products. Termination probability was calculated by determining the number of molecules within the $[GT]_{10}$ microsatellite divided by the number of molecules within and 3' to the $[GT]_{10}$ microsatellite. Graphs compare results from equal activities of Pol κ and Pol $\delta 4$. Data points are the mean of 2–6 independent reactions; error bars represent the standard deviation determined from 3 or more reactions.

little as 40 fmol Pol κ (Figure 5B). The presence of PCNA did not affect the results in either set of experiments, indicating that PCNA does not inhibit the competition between Pols $\delta 4$ and κ (Figure 5). These biochemical results suggest that Pols $\delta 4$ and κ can act cooperatively to reduce polymerase stalling within microsatellite sequences.

DISCUSSION

Intrinsic DNA features have been established as the primary determinants of microsatellite allele length variation (33). While the strand-slippage mechanism can readily account for the effects of microsatellite length (number of repeat units) on mutability, the mechanisms by which motif size and sequence composition affect microsatellite variation are less well established. In this study, we report that the human Y-family polymerase, Pol κ , displays a high accuracy during dinucleotide microsatellite DNA synthesis. Surprisingly, we observed that

the relative DNA polymerase accuracy for unit-based indel errors during dinucleotide microsatellite DNA synthesis is: Pol $\kappa \geq$ Pol $\delta 4 >$ Pol η (Figure 3C, D). This hierarchy is in distinct contrast to the one we observed within the HSV-tk-coding sequence control: Pol $\delta 4 \gg$ Pol κ or Pol η . Although Pol κ generated many strand-slippage errors within mononucleotide repeats, it is unusually accurate for unit-based indel events at the dinucleotide microsatellites (Figure 3). This behavior contrasts not only with human Pol $\delta 4$, but also with yeast Pol δ and Pol ϵ holoenzymes, and calf-thymus Pol α -primase (Table 3). We measured a significantly higher termination probability for Pol $\delta 4$ than for Pol κ within the $[GT]_{10}$ microsatellite (Figure 4), and used this differential termination to demonstrate that Pol κ can compete with a moving Pol $\delta 4$ enzyme during microsatellite DNA synthesis (Figure 5). These results demonstrate that Pol $\delta 4$ and Pol κ can cooperate enzymatically during dinucleotide microsatellite DNA synthesis. Our study conceptually extends the role of Pol κ beyond accurate translesion

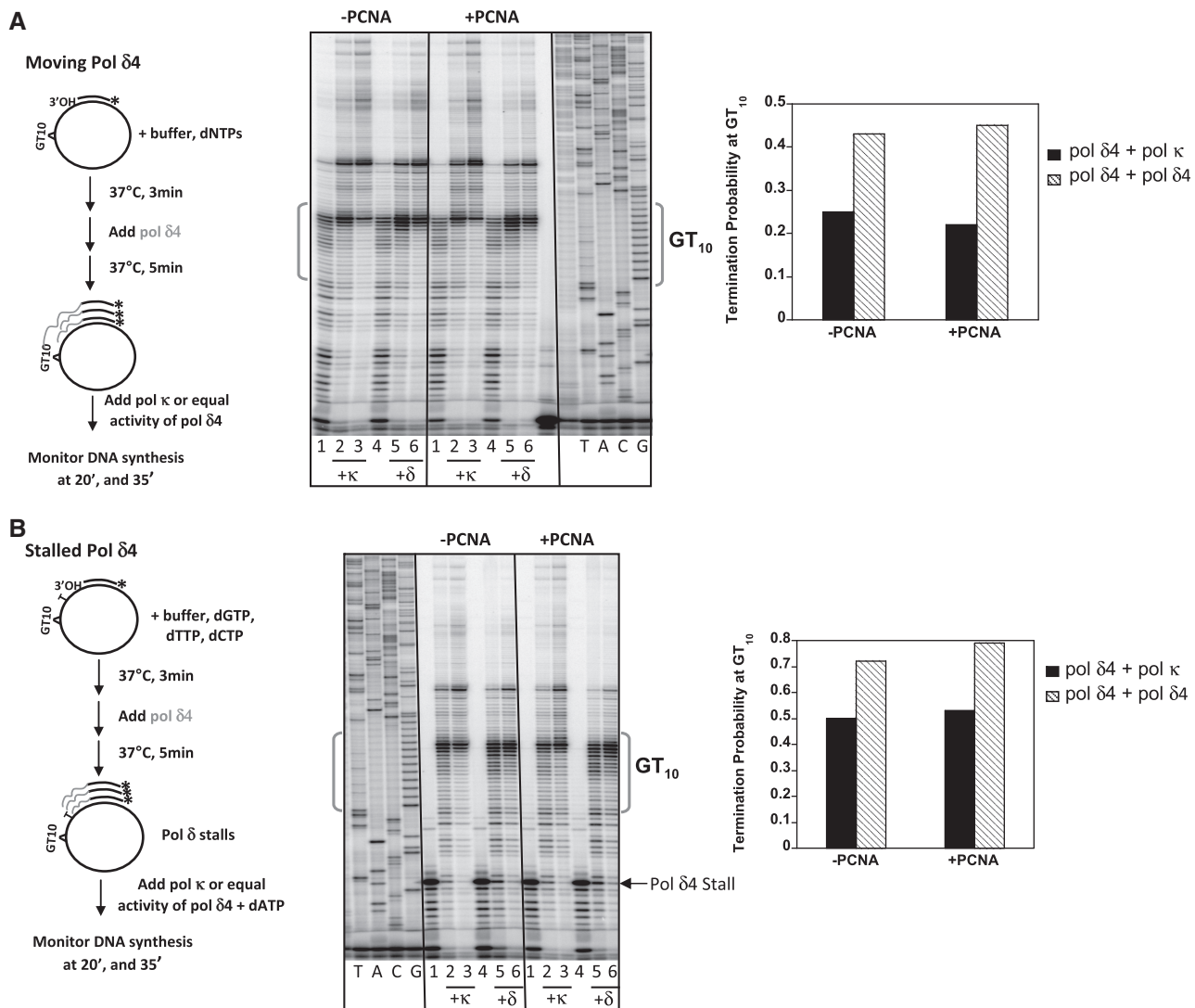


Figure 5. Pol κ and Pol δ 4 act cooperatively to alleviate pausing within the [GT]₁₀ microsatellite. (A) Analyses performed under moving Pol δ 4 conditions. *Left panel:* Schematic of the experimental design. *Middle panel:* Phosphoimager scan of reaction products obtained in either the absence (–PCNA) or presence (+PCNA) of 500 fmol PCNA. Lanes 1 and 4 of each reaction set show products after the 5 min incubation with 400 fmol Pol δ 4 alone. Lanes 2 and 3 are products after addition of 40 fmol of Pol κ . The reactions were terminated after an additional 20 or 35 min. Lanes 5 and 6 are products after second addition of Pol δ 4 (200 fmol for a total of 600 fmol) and termination after an additional 20 or 35 min. Polymerase conditions were chosen so that 100% of the available primer-template was extended by 20 min whether we added Pol κ or additional Pol δ 4. *Right panel:* Termination probability within the [GT]₁₀ sequence at 35 min under each polymerase condition. (B) Analyses performed under stalled Pol δ 4 conditions. Pol δ 4 stalling was created by excluding dATP during the first 5 min of the reaction. Reactions conditions are otherwise the same as in (A).

synthesis to include accurate synthesis of dinucleotide repetitive elements. As other studies (refs. 15–18) also have indicated a more widespread functional role of Y-family polymerases, we propose that the terminology ‘specialized polymerases’ to describe the Y-family polymerases may be more appropriate than the term TLS polymerases. Our data also demonstrate that the broad characterization of Y-family polymerases as error prone is not appropriate when considering the entire genome.

Pol κ could potentially promote microsatellite stability in two ways. First, this polymerase has an inherently high fidelity for unit-based indel errors within dinucleotide microsatellites (Figure 3C, D), and may act to limit microsatellite allele length variation. Second, when Pol κ does

make errors within the microsatellites, it frequently creates interruption errors (Figure 2) within the long tandem repeat. We reported previously that a threshold length of 5 units exists for the mutability of GT/CA microsatellites *in vitro* and in human populations (34). Below the threshold length, the rate of mutation within the tandem repeat is not higher than the rate of indel mutations in coding sequences. Above the threshold, the mutability of the tandem repeat increases exponentially as the number of repeats increases. Therefore, the interruption errors made by Pol κ effectively break the long dinucleotide repeat arrays into two, shorter arrays that will mutate at a lower frequency. The *in vitro* results we report here are entirely consistent with the *in vivo* phenotype of Pol κ null

mice. The spontaneous germline mutation rate within two expanded short tandem repeat (ESTR) alleles for Pol κ -deficient mice is significantly higher than within isogenic Pol κ wild-type mice (18).

All cells contain multiple DNA polymerases, and a widely held belief is that individual polymerases serve specialized functions that are necessary to maintain genome stability (19). The original paradigm for the functions of TLS polymerases posited that these enzymes promote the bypass of DNA lesions representing severe obstacles to replicative DNA polymerases, albeit at the cost of introducing mutations (37). This paradigm has shifted, as additional evidence has demonstrated that TLS polymerases can carry out error free bypass of specific DNA lesions *in vivo*, suggesting that this group of polymerases are structurally adapted for cognate lesions (38,39). Specifically, Pol κ has been implicated in efficient and error-free bypass *in vivo* of exocyclic N²-guanine lesions, such as benzo(a)pyrene diol epoxide formed by polycyclic aromatic hydrocarbons (PAH) (13,40).

The studies we report here extend this growing paradigm shift, with the novel finding that Pol κ is accurate when processing dinucleotide repetitive elements. The number of dinucleotide microsatellite alleles in the human reference genome (hg 18) is ~227 000 for [GT/CA] alleles alone, and ~500 000 for dinucleotide alleles of all sequence motifs (Supplementary Table S2). In comparison, the number of PAH adducts present in the genomes of mothers and newborns (41) or non-smokers (42) is 78–1080 adducts/cell, and rises to a high of 2040 adducts/cell in the lung epithelium of smokers (42). Clearly, the potential mutational load from polymerase errors during synthesis of microsatellite sequences in the human genome is much higher than that expected from PAH lesions. The exact role of Pol κ in genome replication will need to be investigated by additional *in vivo* studies.

The proposal that specialized polymerases, such as Pol κ , participate in chromosomal replication to maintain genomic integrity implies that genome-wide replication involves the cooperation of multiple DNA polymerases in addition to the classical replicative polymerases. In eukaryotes, a direct interaction has been shown between Rev1 and the Pol δ Pol32 subunit (43) as well as between Rev1 and Pol κ (44), consistent with models proposing that TLS polymerases may be an integral component of the replication fork. Indeed, human Pol κ can be found localized to PCNA-containing replication foci in undamaged cells (45). Current models of *E. coli* replication also propose the presence of multiple DNA polymerases at the replication fork. The active *E. coli* replisome has been shown by direct microscopy in living cells to contain three molecules of the replicative polymerase (46). In a biochemical study investigating the roles of Pol II and Pol IV outside of TLS, both polymerases were shown to have access to the DNA replication fork, and to freely exchange with Pol III in a moving replisome (35). The suggestion has been made that the third polymerase of the *E. coli* replisome may act as a reserve polymerase to assist during replication fork stalling, and that

Pol II and Pol IV occupy the replisome to some extent during normal cellular growth (47). Thus, there exists the potential that specialized polymerases may encompass a role in replication at specific DNA structural elements. Our biochemical study (Figure 5) is similar to the previous analyses of replicative and Y-family DNA polymerase exchange (35,36,48), and extends this phenomenon to now include human Pol δ 4 in addition to replicative polymerases of *E. coli*, T4 bacteriophage, and *S. cerevisiae*. Additionally, we are the first to provide evidence that Pol κ participates in an exchange reaction with Pol δ at an undamaged DNA sequence. We observed this exchange in the presence of a moving Pol δ 4 enzyme, similar to what was observed for the *E. coli* Pol IV/Pol III system. Recently, Pol κ was shown to be present in a complex with Pol δ in human cells, and participate in DNA repair synthesis associated with nucleotide excision repair (17).

We presume that the differential accuracy of Pol κ and Pol δ 4 within mononucleotide and dinucleotide repeats (Figure 3) reflects structural differences between the enzymes that affect utilization of bulged (misaligned) primer templates. Structural information is available for Pols κ and δ in complex with DNA and dNTP substrates (49,50), with the caveat that none of the structures to date correspond to the full length, wild-type (and for Pol δ , multisubunit) enzymes we have used in this study. The unique N-clasp interaction of Pol κ locks the polymerase around the DNA substrate, creating a restrictive active site (50). We found that Pol κ is accurate during synthesis of dinucleotide repeats, but inaccurate for mononucleotide repeats. Possibly, the intimate Pol κ interactions with the nascent basepair and unpaired nucleotides 5' to the templating base may disfavor utilization of bulges greater than one nucleotide. Alternatively, the N-clasp may cause Pol κ to have a novel interaction with the templating strand, such that the enzyme does not sense the entirety of the long tandem dinucleotide repeat during DNA synthesis, but instead only reads the template one base at a time. This model would account for the unique pattern of interruption mutations (primarily, single base insertions or deletions) produced by Pol κ within the dinucleotide repeats. Pol δ , which primarily creates unit-based (two nucleotide) indels within the microsatellite, has a much larger protein footprint along the template strand through interactions of the N-terminal domain and the exonuclease domain (49). Such interactions of Pol δ may provide stabilizing contacts for looped out/bulged bases in the template strand, analogous to the stabilizing protein-extrahelical base interactions observed in the Dbh4 and Dpo4 polymerase-strand misalignment structures (51,52).

Microsatellite allele length variation, or microsatellite instability, is associated with 10–15% of colorectal, endometrial and gastric cancers, and has long been used as a diagnostic tool for Lynch Syndrome cancers. Alterations within microsatellites are generally accepted to be a consequence of strand slippage events during DNA replication that are left uncorrected by a defective mismatch repair system. Tumors of this type are characterized as MSI-High, with mononucleotide microsatellite markers

proving to be more sensitive and predictive for Lynch Syndrome than dinucleotide markers (53). In addition, a group of sporadic colorectal carcinomas have been consistently identified, termed MSI-Low. The underlying cause of the MSI-Low phenotype is controversial, and it is unknown whether MSI-Low represents random mutations arising during clonal tumor cell evolution, or represents a mild mutator phenotype resulting from loss of a genome stability factor distinct from MMR (54–56). However, over- or under-expression of repair factors, such as alkyladenine DNA glycosylase (57) and methylguanine DNA methyltransferase (58), can contribute to an MSI-Low phenotype. Intriguingly, decreased Pol κ expression has been reported in colorectal tumors (59,60), relative to adjacent normal tissue. Results from our study and others may help to uncover unknown susceptibility factors in cancers exhibiting microsatellite instability.

SUPPLEMENTARY DATA

Supplementary Data are available at NAR online.

ACKNOWLEDGEMENTS

We thank Mr. Guruprasad Ananda (Penn State University, Center for Comparative Genomics and Bioinformatics) for providing us with the human genome microsatellite enumeration data. We thank Drs. Joann Sweasy and Laura Carrel, and members of the Eckert laboratory for critical discussions and reading of the manuscript.

FUNDING

National Institutes of Health (grant numbers GM31973, ES014737 to M.Y.W.T.L., and CA100060, GM87472 to K.A.E.), and by generous contributions to the Gittlen Cancer Research Foundation of Penn State University. Funding for open access charge: National Institutes of Health (grant number GM87472 to K.A.E.)

Conflict of interest statement. None declared.

REFERENCES

- Richard, G.F., Kerrest, A. and Dujon, B. (2008) Comparative genomics and molecular dynamics of DNA repeats in eukaryotes. *Microbiol. Mol. Biol. Rev.*, **72**, 686–727.
- Subramanian, S., Mishra, R.K. and Singh, L. (2003) Genome-wide analysis of microsatellite repeats in humans: their abundance and density in specific genomic regions. *Genome Biol.*, **4**, R13.
- Gemayel, R., Vines, M.D., Legendre, M. and Verstrepen, K.J. (2010) Variable tandem repeats accelerate evolution of coding and regulatory sequences. *Annu. Rev. Genet.*, **44**, 445–477.
- Hefferon, T.W., Groman, J.D., Yurk, C.E. and Cutting, G.R. (2004) A variable dinucleotide repeat in the CFTR gene contributes to phenotype diversity by forming RNA secondary structures that alter splicing. *Proc. Natl Acad. Sci. USA*, **101**, 3504–3509.
- Gangwal, K., Sankar, S., Hollenhorst, P.C., Kinsey, M., Haroldsen, S.C., Shah, A.A., Boucher, K.M., Watkins, W.S., Jorde, L.B., Graves, B.J. *et al.* (2008) Microsatellites as EWS/FLI response elements in Ewing's sarcoma. *Proc. Natl Acad. Sci. USA*, **105**, 10149–10154.
- Mirkin, S.M. (2007) Expandable DNA repeats and human disease. *Nature*, **447**, 932–940.
- Waters, L.S., Minesinger, B.K., Wiltrout, M.E., D'Souza, S., Woodruff, R.V. and Walker, G.C. (2009) Eukaryotic translesion polymerases and their roles and regulation in DNA damage tolerance. *Microbiol. Mol. Biol. Rev.*, **73**, 134–154.
- Sweasy, J.B., Lauper, J.M. and Eckert, K.A. (2006) DNA polymerases and human diseases. *Radiat. Res.*, **166**, 693–714.
- Ohmori, H., Friedberg, E.C., Fuchs, R.P., Goodman, M.F., Hanaoka, F., Hinkle, D., Kunkel, T.A., Lawrence, C.W., Livneh, Z., Nohmi, T. *et al.* (2001) The Y-family of DNA polymerases. *Mol. Cell*, **8**, 7–8.
- Masutani, C., Kusumoto, R., Yamada, A., Dohmae, N., Yokoi, M., Yuasa, M., Araki, M., Iwai, S., Takio, K. and Hanaoka, F. (1999) The XPV (xeroderma pigmentosum variant) gene encodes human DNA polymerase η . *Nature*, **399**, 700–704.
- Johnson, R.E., Washington, M.T., Prakash, S. and Prakash, L. (2000) Fidelity of human DNA polymerase η . *J. Biol. Chem.*, **275**, 7447–7450.
- Masutani, C., Kusumoto, R., Iwai, S. and Hanaoka, F. (2000) Mechanisms of accurate translesion synthesis by human DNA polymerase η . *Embo. J.*, **19**, 3100–3109.
- Avkin, S., Goldsmith, M., Velasco-Miguel, S., Geacintov, N., Friedberg, E.C. and Livneh, Z. (2004) Quantitative analysis of translesion DNA synthesis across a benzo[a]pyrene-guanine adduct in mammalian cells: the role of DNA polymerase κ . *J. Biol. Chem.*, **279**, 53298–53305.
- Jarosz, D.F., Godoy, V.G., Delaney, J.C., Essigmann, J.M. and Walker, G.C. (2006) A single amino acid governs enhanced activity of DinB DNA polymerases on damaged templates. *Nature*, **439**, 225–228.
- Rey, L., Sidorova, J.M., Puget, N., Boudsocq, F., Biard, D.S., Monnat, R.J. Jr, Cazaux, C. and Hoffmann, J.S. (2009) Human DNA polymerase η is required for common fragile site stability during unperturbed DNA replication. *Mol. Cell. Biol.*, **29**, 3344–3354.
- Betous, R., Rey, L., Wang, G., Pillaire, M.J., Puget, N., Selves, J., Biard, D.S., Shin-ya, K., Vasquez, K.M., Cazaux, C. *et al.* (2009) Role of TLS DNA polymerases η and κ in processing naturally occurring structured DNA in human cells. *Mol. Carcinog.*, **48**, 369–378.
- Ogi, T., Limsirichaikul, S., Overmeer, R.M., Volker, M., Takenaka, K., Cloney, R., Nakazawa, Y., Niimi, A., Miki, Y., Jaspers, N.G. *et al.* (2010) Three DNA polymerases, recruited by different mechanisms, carry out NER repair synthesis in human cells. *Mol. Cell*, **37**, 714–727.
- Burr, K.L., Velasco-Miguel, S., Duvvuri, V.S., McDaniel, L.D., Friedberg, E.C. and Dubrova, Y.E. (2006) Elevated mutation rates in the germline of Polkappa mutant male mice. *DNA Repair*, **5**, 860–862.
- Bebenek, K. and Kunkel, T.A. (2004) Functions of DNA polymerases. *Adv. Protein Chem.*, **69**, 137–165.
- Fortune, J.M., Pavlov, Y.I., Welch, C.M., Johansson, E., Burgers, P.M. and Kunkel, T.A. (2005) *Saccharomyces cerevisiae* DNA polymerase delta: high fidelity for base substitutions but lower fidelity for single- and multi-base deletions. *J. Biol. Chem.*, **280**, 29980–29987.
- Korona, D.A., Lecompte, K.G. and Pursell, Z.F. (2010) The high fidelity and unique error signature of human DNA polymerase epsilon. *Nucleic Acids Res.*, **39**, 1763–1773.
- Abdulovic, A.L., Hile, S.E., Kunkel, T.A. and Eckert, K.A. (2011) The *in vitro* fidelity of yeast DNA polymerase delta and polymerase varepsilon holoenzymes during dinucleotide microsatellite DNA synthesis. *DNA Repair*, **10**, 497–505.
- Xie, B., Mazloun, N., Liu, L., Rahmeh, A., Li, H. and Lee, M.Y. (2002) Reconstitution and characterization of the human DNA polymerase delta four-subunit holoenzyme. *Biochemistry*, **41**, 13133–13142.
- Eckert, K.A., Mowery, A. and Hile, S.E. (2002) Misalignment-mediated DNA polymerase beta mutations: comparison of microsatellite and frame-shift error rates using a forward mutation assay. *Biochemistry*, **41**, 10490–10498.

25. Hile, S.E. and Eckert, K.A. (2008) DNA polymerase kappa produces interrupted mutations and displays polar pausing within mononucleotide microsatellite sequences. *Nucleic Acids Res.*, **36**, 688–696.
26. Eckert, K.A., Hile, S.E. and Vargo, P.L. (1997) Development and use of an *in vitro* HSV-tk forward mutation assay to study eukaryotic DNA polymerase processing of DNA alkyl lesions. *Nucleic Acids Res.*, **25**, 1450–1457.
27. Opreko, P.L., Sweasy, J.B. and Eckert, K.A. (1998) The mutator form of polymerase beta with amino acid substitution at tyrosine 265 in the hinge region displays an increase in both base substitution and frame shift errors. *Biochemistry*, **37**, 2111–2119.
28. Hile, S.E. and Eckert, K.A. (2004) Positive correlation between DNA polymerase alpha-primase pausing and mutagenesis within polypyrimidine/polypurine microsatellite sequences. *J. Mol. Biol.*, **335**, 745–759.
29. Hashimoto, K., Shimizu, K., Nakashima, N. and Sugino, A. (2003) Fidelity of DNA polymerase delta holoenzyme from *Saccharomyces cerevisiae*: the sliding clamp proliferating cell nuclear antigen decreases its fidelity. *Biochemistry*, **42**, 14207–14213.
30. Matsuda, T., Bebenek, K., Masutani, C., Rogozin, I.B., Hanaoka, F. and Kunkel, T.A. (2001) Error rate and specificity of human and murine DNA polymerase eta. *J. Mol. Biol.*, **312**, 335–346.
31. Ohashi, E., Bebenek, K., Matsuda, T., Feaver, W.J., Gerlach, V.L., Friedberg, E.C., Ohmori, H. and Kunkel, T.A. (2000) Fidelity and processivity of DNA synthesis by DNA polymerase kappa, the product of the human DINB1 gene. *J. Biol. Chem.*, **275**, 39678–39684.
32. Schmitt, M.W., Matsumoto, Y. and Loeb, L.A. (2009) High fidelity and lesion bypass capability of human DNA polymerase delta. *Biochimie*, **91**, 1163–1172.
33. Eckert, K.A. and Hile, S.E. (2009) Every microsatellite is different: Intrinsic DNA features dictate mutagenesis of common microsatellites present in the human genome. *Mol. Carcinog.*, **48**, 379–388.
34. Kelkar, Y.D., Strubczewski, N., Hile, S.E., Chiaromonte, F., Eckert, K.A. and Makova, K.D. (2010) What is a microsatellite: a computational and experimental definition based upon repeat mutational behavior at A/T and GT/AC repeats. *Genome Biol. Evol.*, **2**, 620–635.
35. Indiani, C., Langston, L.D., Yurieva, O., Goodman, M.F. and O'Donnell, M. (2009) Translesion DNA polymerases remodel the replisome and alter the speed of the replicative helicase. *Proc. Natl Acad. Sci. USA*, **106**, 6031–6038.
36. Zhuang, Z., Johnson, R.E., Haraeska, L., Prakash, L., Prakash, S. and Benkovic, S.J. (2008) Regulation of polymerase exchange between Pol eta and Pol delta by monoubiquitination of PCNA and the movement of DNA polymerase holoenzyme. *Proc. Natl Acad. Sci. USA*, **105**, 5361–5366.
37. Guo, C., Kosarek-Stancel, J.N., Tang, T.S. and Friedberg, E.C. (2009) Y-family DNA polymerases in mammalian cells. *Cell. Mol. Life Sci.*, **66**, 2363–2381.
38. Friedberg, E.C., Wagner, R. and Radman, M. (2002) Specialized DNA polymerases, cellular survival, and the genesis of mutations. *Science*, **296**, 1627–1630.
39. Takata, K. and Wood, R.D. (2009) Bypass specialists operate together. *EMBO J.*, **28**, 313–314.
40. Ogi, T., Shinkai, Y., Tanaka, K. and Ohmori, H. (2002) Pol kappa protects mammalian cells against the lethal and mutagenic effects of benzo[a]pyrene. *Proc. Natl Acad. Sci. USA*, **99**, 15548–15553.
41. Perera, F., Hemminki, K., Jedrychowski, W., Whyatt, R., Campbell, U., Hsu, Y., Santella, R., Albertini, R. and O'Neill, J.P. (2002) In utero DNA damage from environmental pollution is associated with somatic gene mutation in newborns. *Cancer Epidemiol. Biomarkers Prev.*, **11**, 1134–1137.
42. Phillips, D.H., Hewer, A., Martin, C.N., Garner, R.C. and King, M.M. (1988) Correlation of DNA adduct levels in human lung with cigarette smoking. *Nature*, **336**, 790–792.
43. Acharya, N., Johnson, R.E., Pages, V., Prakash, L. and Prakash, S. (2009) Yeast Rev1 protein promotes complex formation of DNA polymerase zeta with Pol32 subunit of DNA polymerase delta. *Proc. Natl Acad. Sci. USA*, **106**, 9631–9636.
44. Ohashi, E., Hanafusa, T., Kamei, K., Song, I., Tomida, J., Hashimoto, H., Vaziri, C. and Ohmori, H. (2009) Identification of a novel REV1-interacting motif necessary for DNA polymerase kappa function. *Genes Cells*, **14**, 101–111.
45. Bergoglio, V., Bavoux, C., Verbiest, V., Hoffmann, J.S. and Cazaux, C. (2002) Localisation of human DNA polymerase kappa to replication foci. *J. Cell Sci.*, **115**, 4413–4418.
46. Reyes-Lamothe, R., Sherratt, D.J. and Leake, M.C. (2010) Stoichiometry and architecture of active DNA replication machinery in *Escherichia coli*. *Science*, **328**, 498–501.
47. Langston, L.D., Indiani, C. and O'Donnell, M. (2009) Whither the replisome: emerging perspectives on the dynamic nature of the DNA replication machinery. *Cell Cycle*, **8**, 2686–2691.
48. Yang, J., Zhuang, Z., Roccasecca, R.M., Trakselis, M.A. and Benkovic, S.J. (2004) The dynamic processivity of the T4 DNA polymerase during replication. *Proc. Natl Acad. Sci. USA*, **101**, 8289–8294.
49. Swan, M.K., Johnson, R.E., Prakash, L., Prakash, S. and Aggarwal, A.K. (2009) Structural basis of high-fidelity DNA synthesis by yeast DNA polymerase delta. *Nat. Struct. Mol. Biol.*, **16**, 979–986.
50. Lone, S., Townson, S.A., Uljon, S.N., Johnson, R.E., Brahma, A., Nair, D.T., Prakash, S., Prakash, L. and Aggarwal, A.K. (2007) Human DNA polymerase kappa encircles DNA: implications for mismatch extension and lesion bypass. *Mol. Cell*, **25**, 601–614.
51. Wilson, R.C. and Pata, J.D. (2008) Structural insights into the generation of single-base deletions by the Y family DNA polymerase dbh. *Mol. Cell*, **29**, 767–779.
52. Wu, Y., Wilson, R.C. and Pata, J.D. (2011) The Y-family DNA polymerase Dpo4 uses a template slippage mechanism to create single-base deletions. *J. Bacteriol.*, **193**, 2630–2636.
53. Imai, K. and Yamamoto, H. (2008) Carcinogenesis and microsatellite instability: the interrelationship between genetics and epigenetics. *Carcinogenesis*, **29**, 673–680.
54. Halford, S., Sasieni, P., Rowan, A., Wasan, H., Bodmer, W., Talbot, I., Hawkins, N., Ward, R. and Tomlinson, I. (2002) Low-level microsatellite instability occurs in most colorectal cancers and is a nonrandomly distributed quantitative trait. *Cancer Res.*, **62**, 53–57.
55. Jass, J., Whitehall, V., Young, J., Leggett, B., Meltzer, S.J., Matsubara, N. and Fishel, R. (2002) Correspondance re: Laiho *et al.*, Low level microsatellite instability in most colorectal carcinomas. *Cancer Res.*, **62**, 1166–1170, 5988–5990.
56. Laiho, P., Launonen, V., Lahermo, P., Esteller, M., Guo, M., Herman, J.G., Mecklin, J.P., Jarvinen, H., Sistonen, P., Kim, K.M. *et al.* (2002) Low-level microsatellite instability in most colorectal carcinomas. *Cancer Res.*, **62**, 1166–1170.
57. Hofseth, L.J., Khan, M.A., Ambrose, M., Nikolayeva, O., Xu-Welliver, M., Kartalou, M., Hussain, S.P., Roth, R.B., Zhou, X., Mechanic, L.E. *et al.* (2003) The adaptive imbalance in base excision-repair enzymes generates microsatellite instability in chronic inflammation. *J. Clin. Invest.*, **112**, 1887–1894.
58. Whitehall, V.L., Walsh, M.D., Young, J., Leggett, B.A. and Jass, J.R. (2001) Methylation of O-6-methylguanine DNA methyltransferase characterizes a subset of colorectal cancer with low-level DNA microsatellite instability. *Cancer Res.*, **61**, 827–830.
59. Lemeec, F., Bavoux, C., Pillaire, M.J., Bieth, A., Machado, C.R., Pena, S.D., Guimbaud, R., Selves, J., Hoffmann, J.S. and Cazaux, C. (2007) Characterization of promoter regulatory elements involved in downexpression of the DNA polymerase kappa in colorectal cancer. *Oncogene*, **26**, 3387–3394.
60. Pillaire, M.J., Selves, J., Gordien, K., Gourraud, P.A., Gentil, C., Danjoux, M., Do, C., Negre, V., Bieth, A., Guimbaud, R. *et al.* (2010) A 'DNA replication' signature of progression and negative outcome in colorectal cancer. *Oncogene*, **29**, 876–887.